

Metabolic reprogramming by PRDM16 drives cytarabine resistance in acute myeloid leukemia

Junji Ikeda,^{1,2} Hiroyoshi Kunimoto,² Yusuke Saito,³ Shin-Ichi Tsujimoto,¹ Masanobu Takeuchi,¹ Ayaka Miura,² Takayuki Kurosawa,¹ Koichi Murakami,^{4,5} Ikuma Kato,⁶ Megumi Funakoshi-Tago,⁷ Akihiko Yokoyama,⁸ Norio Shiba,¹ Souichi Adachi,⁹ Daisuke Tomizawa,¹⁰ Tomohiko Tamura,⁴ Shuichi Ito¹ and Hideaki Nakajima²

¹Department of Pediatrics, Yokohama City University Graduate School of Medicine, Yokohama; ²Department of Stem Cell and Immune Regulation, Yokohama City University Graduate School of Medicine, Yokohama; ³Division of Clinical Cancer Genomics, Hokkaido University Hospital, Hokkaido; ⁴Department of Immunology, Yokohama City University Graduate School of Medicine, Yokohama; ⁵Division of Hematology, Department of Medicine, Keio University School of Medicine, Tokyo; ⁶Department of Molecular Pathology, Yokohama City University Graduate School of Medicine, Yokohama; ⁷Division of Hygienic Chemistry, Faculty of Pharmacy, Keio University, Tokyo; ⁸Tsuruoka Metabolomics Laboratory, National Cancer Center, Yamagata; ⁹Human Health Science, Graduate School of Medicine, Kyoto University, Kyoto and ¹⁰Division of Leukemia and Lymphoma, Children's Cancer Center, National Center for Child Health and Development, Tokyo, Japan

Correspondence: H. Kunimoto
kunimoto@yokohama-cu.ac.jp

H. Nakajima
hnakajim@yokohama-cu.ac.jp

Received: December 24, 2024.
Accepted: May 23, 2025.
Early view: June 12, 2025.

<https://doi.org/10.3324/haematol.2024.287265>

©2025 Ferrata Storti Foundation

Published under a CC BY-NC license



Supplemental Information

Supplemental Methods

Retrovirus vectors

The retroviral vectors pMSCV-GFP-short isoform mouse Prdm16 and pMSCV-GFP-short isoform human PRDM16 have been described previously and were kindly provided by Dr. Saito.¹³ pMSCV-DsRedExpress2-MLL::AF9 (Plasmid #71444) and pMSCV-GFP-Myc (Plasmid #35396) were purchased from Addgene (MA, USA). pMSCV-neomycin-MLL::AF9 have been described previously and were kindly provided by Dr. Yokoyama.¹

Retroviral transduction

Plat-E cells were transiently transfected with each MSCV vector to generate retroviral supernatant. Whole bone marrow cells were harvested from C57BL/6 or Flt3^{ITD} mice, and c-Kit positive cells were subsequently isolated using EasySep Mouse CD117 Positive Selection Kit (STEMCELL Technologies, Vancouver, Canada). These cells were incubated in S-Clone SF-O3 medium (Iwai North America, CA, USA) supplemented with 0.1% BSA, 100 ng/ml mouse SCF, and 100 ng/ml mouse TPO. After 24 hours, the cells were spin-infected with retroviral supernatant supplemented with 8 µg/ml polybrene at 2000 rpm for 90 minutes at room temperature. We sorted DsRed-positive and GFP-positive cells transduced with MLL::AF9- and sPrdm16-expressing vectors using BD FACS Aria II (Becton Dickinson, NJ, USA).

Gene Knockdown with lentiviral shRNA vectors

Lentiviral shRNA vectors targeting mouse c-Myc were purchased from VectorBuilder Japan (Yokohama, Japan). The target sequences of the shRNA are as follows: #1; 5'-GACTCCGTACAGCCCTATTTTC-3' (#VB900137-9790npj) and #2; 5'-ATCATCATCCAGGACTGTATG-3' (#VB900124-8491hbu). These vectors were transfected into Lenti-X 293T cells with pMD2.G containing VSV-G and psPAX2 containing Gag, Pol, Rev, and Tat genes. MA9/sPrdm16 cells were infected with the lentiviral supernatant and selected by exposure to 2 µg/ml puromycin for 72 hours.

Quantitative reverse transcription PCR analysis

Total RNA was extracted from murine AML cells established in this study using RNeasy Mini Kit (Qiagen, Venlo, Netherland) according to manufacturer's instructions. cDNA was synthesized

using ReverTra Ace qPCR RT Master Mix (TOYOBO, Osaka, Japan). Quantitative RT-PCR was performed using THUNDERBIRD SYBR qPCR Mix (TOYOBO, Osaka, Japan) and CFX96 Touch Deep Well Real-Time PCR System (Bio-Rad, Hercules, CA, USA). Relative mRNA expression normalized to housekeeping genes was analyzed by the Δ CT method. The sequences of the primers for each gene are as follows: mouse Prdm16 (Forward: 5'-CTCCGAGATCCGAACTTCA-3', Reverse: 5'-CAGCTCCTCTCTTCCTCCT-3'), mouse c-Myc (Forward: 5'-ATCAGCAACAACCGCAAGTG-3', Reverse: 5'-TGTGCTCGTCTGCTTGAATG-3'), and mouse β -actin (internal control) (Forward: 5'-GATCTGGCACCACACCTTCT-3', Reverse: 5'-CCATCACAATGCCTGTGGTA-3'). These PCR primers were purchased from Eurofins Genomics (Tokyo, Japan).

RNA sequencing

WT/control and WT/sPrdm16 cells were seeded into Methocult M3434 methylcellulose medium and incubated at 37°C in a humidified atmosphere with 5% CO₂ for 7 days. These cells were harvested, and the CD11b-positive fraction was sorted using FACS Aria II. Total RNA was extracted using RNeasy Mini Kit (Qiagen, Venlo, Netherland). Quality control of RNA sample was performed using the TapeStation or BioAnalyzer (Agilent Technologies, CA, USA). cDNA was synthesized with the SMART-Seq v4 Ultra Low Input RNA Kit for Sequencing (Clontech, CA, USA) and sequence library was prepared using Nextera XT DNA Library Prep Kit and Nextera XT Index Kit v2 SetA/B/C/D (Illumina, CA, USA) according to the manufacturer's instructions. Sequencing was performed using an Illumina NovaSeq 6000 sequencer (150 bp paired-end runs). The raw sequencing data were converted to fastq files and aligned to the mouse reference genome (GRCm38) using DRAGEN Bio-IT Platform version 3.6.3 (Illumina, CA, USA). Differentially expressed genes (DEGs) between control and sPrdm16 high expression cells were analyzed. The Benjamini & Hochberg procedure was used to control the false discovery rate (FDR). Gene Ontology (GO) analysis was performed with DAVID, a web-based bioinformatics resource (<https://david.ncifcrf.gov/>). RNA-seq data are available at GEO under accession number GSE280735.

Gene set enrichment analysis (GSEA)

GSEA was performed as previously described.² Gene sets were obtained from the Molecular Signatures Database (MSigDB) available on the GSEA website (<https://www.gsea-msigdb.org/gsea/msigdb/index.jsp>).

Western Blotting

MA9/control and MA9/sPrdm16, MA9/control and MA9/c-Myc, MOLM-13/control and MOLM-13/sPRDM16, or THP-1/control and THP-1/sPRDM16 cells (1.0×10^7 cells) were lysed with RIPA buffer, and total protein lysate was denatured at 100°C for 5 minutes. 5–20 µg of each protein was separated by SDS-PAGE at 120V and transferred onto PVDF membranes (Merck Millipore, MA, USA) using a wet transfer system at 30V for 60 minutes at 4°C. After transfer, the membranes were blocked in Blocking Reagent (TOYOBO, Osaka, Japan) for 1 hour at room temperature. The membranes were then incubated with the primary antibody overnight at 4°C with gentle shaking. After washing, the membranes were incubated with the secondary antibody for 1 hour at room temperature. After washing, the chemiluminescent signal visualized by ECL reaction was detected using ImageQuant LAS 500 (GE Healthcare Life Science, Uppsala, Sweden). The following antibodies were used for western blotting: Prdm16 (Novus Biologicals, CO, USA), c-Myc (Cell Signaling, MA, USA), Slc1a5 (Cell Signaling, MA, USA), β-actin (BioLegend, CA, USA), and Vinculin (Cell Signaling, MA, USA).

Flow cytometric analysis

For immunophenotyping, murine AML cells were stained with APC/Cyanine7-conjugated Gr-1 (Clone RB6-8C5), Pacific Blue-conjugated CD11b (M1/70), Brilliant Violet 605-conjugated c-kit (ACK2), APC-conjugated CD3 (17A2), and PE/Cyanine7-conjugated B220 antibody (RA3-6B2) (All from BioLegend, CA, USA) in FACS buffer for 30 minutes on ice. For cell cycle analysis, these cells were fixed and permeabilized using FIX & PERM Fixation and Permeabilization Kit (Invitrogen, MA, USA). Subsequently, these cells were stained with PerCP/Cyanine5.5-conjugated mouse Ki-67 antibody (B56) (BD Biosciences, NJ, USA) and DAPI. To measure mitochondrial reactive oxygen species (ROS), mass, and membrane potential, murine AML cells were stained with 5 µM MitoSOX for 10 minutes, 50 nM MitoTracker Deep Red for 15 minutes, and 25 nM tetramethylrhodamine methyl ester (TMRM) for 30 minutes at 37°C in the dark, respectively. These cells were analyzed on BD FACSCelesta flow cytometer (Becton Dickinson, NJ, USA). All data were analyzed with FlowJo 10 (Tree Star, NJ, USA).

Colony forming assays

Murine AML cells were plated in Methocult M3434 methylcellulose medium (STEMCELL Technologies, Vancouver, Canada) at 1.0×10^4 cells per well in triplicate. These cells were

incubated at 37°C in a humidified atmosphere with 5% CO₂ for 7 days, and the colony number was subsequently counted.

Cell viability assay

Murine AML cells were plated at a density of 1.0×10^4 cells per well in a 96 well plate and exposed to various concentrations of cytarabine or daunorubicin. AraC (Toronto Research Chemicals, Vaughan, Canada) was serially diluted to 0, 1, 10, 25, 50, 100, 250, 500, 1000, and 5000 nM, and DNR (FUJIFILM Wako Chemicals, Osaka, Japan) was diluted to 0, 1, 5, 7.5, 10, 12.5, 15, 20, 25, and 100 nM. In combination with AraC, the following agents were used: metformin (Sigma-Aldrich, MO, USA), tigecycline (Sigma-Aldrich, MO, USA), IACS-010759 (Selleck, TX, USA), BPTES (Selleck, TX, USA), and 10058-F4 (Selleck, TX, USA). Relative cell viability compared to vehicle-treated controls was evaluated after 72 hours using CellTiter-Glo 2.0 Cell Viability Assay (Promega, WI, USA) according to the manufacturer's instructions. Luciferase signals were measured using POWERSCAN HT Microplate Reader (BioTek, VT, USA). Dimethyl sulfoxide (DMSO) was used as a vehicle.

Evaluation of synergistic effect in multi-drug combination

The synergistic effect was analyzed using the Highest Single Agent (HSA) model through SynergyFinder web application (<https://synergyfinder.fimm.fi>).

Measurement of oxygen consumption rate and extracellular acidification rate (Seahorse assay)

Oxygen consumption rate (OCR) and extracellular acidification rate (ECAR) were measured using Extracellular XFe96 flux analyzer (Agilent Technologies, CA, USA) according to manufacturer's protocols. Murine AML cells were suspended in Seahorse XF RPMI Medium containing 10mM Glucose, 1mM Pyruvate, and 2mM L-Glutamine. These cells were seeded at 1.0×10^5 cells per well on Seahorse XFe96 microplates coated with Cell-Tak at a concentration of 22.4µg/ml. In the Mito Stress test, we measured OCR at basal respiration, respiration linked to ATP production, maximal respiration, and non-mitochondrial respiration under basal conditions and following the injection of 1.5 µM oligomycin, 1.0 µM FCCP, and 0.5 µM Rotenone/antimycinA, respectively. In the Glycolysis Stress Test, ECAR was measured to assess glycolysis, glycolytic capacity and reserve, and non-glycolytic acidification following the injection of 10 mM glucose, 1.0 µM oligomycin, and 50 mM 2-DG, respectively.

Capillary electrophoresis time-of-flight mass spectrometry-based metabolome profiling

MA9/sPrdm16 and MA9/control cells were exposed to either vehicle (DMSO) or 500 nM cytarabine for 1 hour. The cells were harvested, washed with PBS, and then washed with 5% mannitol. Subsequently, the cells were suspended in methanol containing 200 μ M morpholinoethanesulfonic acid and 200 μ M methionine sulfone. After sonication on ice, chloroform was added to the supernatant, and the mixture was then centrifuged at 15,000 rpm for 15 minutes at 4°C. The supernatant was filtered through the 5kDa cutoff filter (UFC3LCCNB, Human Metabolome Technologies, Tsuruoka, Japan) at 10,000 \times g for 15 minutes at 4°C, and the metabolites were then analyzed using the Agilent CE time-of-flight MS system.

Glutamine/Glutamate-Glo Assay

To measure the intracellular glutamine and glutamate levels, we used Glutamine/Glutamate-Glo Assay kit (Promega, WI, USA) according to manufacturer's instructions. Briefly, 1.5×10^5 cells suspended in PBS were seeded into a 96-well plate. Luciferase signals were measured using POWERSCAN HT Microplate Reader (BioTek, VT, USA). The glutamine level was calculated by subtracting glutamate level from total levels of glutamine and glutamate.

Bone marrow transplantation

Female C57BL/6-Ly5.1 (CD45.1) mice aged 7–10 weeks were sub-lethally irradiated (6.0Gy) using MBR-1520R-4 (HITACHI Power Solutions, Ibaraki, Japan). MA9/control or MA9/sPrdm16 cells were transplanted into these mice at $1.0\text{--}5.0 \times 10^4$ cells per mouse via tail vein injection. In order to confirm the engraftment of these cells and the development of AML, peripheral blood chimerism of mouse CD45.2⁺ cells was measured using flow cytometry.

Statistical analysis

Statistical analysis was performed using the two-tailed unpaired Student's t test, the Mann-Whitney U test, or log-rank test with GraphPad Prism 9 software (CA, USA). Group data are represented as mean \pm standard deviation for the two-tailed unpaired Student's t test. P-value < 0.05 was considered to be statistically significant.

References

1. Yokoyama A, Lin M, Naresh A, et al. A higher-order complex containing AF4 and ENL family proteins with P-TEFb facilitates oncogenic and physiologic MLL-dependent transcription. *Cancer Cell*. 2010; 17(2):198-212.

2. Subramanian A, Tamayo P, Mootha VK, et al. 14 Gene set enrichment analysis: a knowledge-based approach for interpreting 15 genome-wide expression profiles. *Proc Natl Acad Sci USA*. 2005; 102(43):15545-15550.

Supplemental Figure legends

Supplemental Figure 1. Characterization of *WT* or *MLL::AF9* leukemia cells transduced with *sPrdm16*-expressing vector.

(A) Relative *Prdm16* expression in *WT/control* and *WT/sPrdm16* cells was measured by quantitative reverse transcription PCR (qRT-PCR) (n=3 for each group).

(B) Growth curve of *WT/control* and *WT/sPrdm16* cells (n=3 for each group). *WT/sPrdm16* cells acquired significant proliferative capacity compared to *WT/control* cells at each time point. Cells were cultured in RPMI + 10% fetal bovine serum (FBS) + 5ng/mL of interleukin-3 (IL-3).

(C) Colony forming assay was performed using *WT/control* and *WT/sPrdm16* cells, which were plated in triplicate.

(D) Relative *Prdm16* expression in *MA9/control* and *MA9/sPrdm16* cells was measured by qRT-PCR (n=3 for each group).

(E) Representative immunophenotype of *MA9/control* and *MA9/sPrdm16* cells.

(F) Growth curve of *MA9/control* and *MA9/sPrdm16* cells (n=3 for each group).

(G) Kaplan-Meier survival curve of *MA9/control* (N=10) and *MA9/sPrdm16* mice (N=10). 5.0×10^4 leukemia cells were transplanted to each sublethally irradiated (6.0Gy) recipient mouse.

(H) Representative images of Wright-Giemsa staining of bone marrow cells derived from *MA9/control* (upper panel) and *MA9/sPrdm16* mice (lower panel).

All data are represented as mean \pm standard deviation. An unpaired Student's t test was used to calculate p values. The log rank test was used in survival time analysis. N.S., not significant; **<0.01; ***<0.001; ****<0.0001; *****<0.00001.

Supplemental Figure 2. *sPRDM16* induces cytarabine resistance in *WT* and *Flt3^{ITD}* cells in a cell cycle-independent manner.

(A) In vitro drug sensitivity assay for cytarabine using *WT/control* and *WT/sPrdm16* (n=3 for each group). RPMI + 10%FBS + 7ng/mL of IL-3 + 10ng/mL of IL-6 + 10ng/mL of stem cell factor (SCF) was used for cell culture.

(B) Colony forming assays with cytarabine (left panel) or daunorubicin (right panel) were

performed using *WT/control* and *WT/sPrdm16* cells, which were plated in triplicate. Methocult M3434 methylcellulose medium was used for cell culture, which contains IL-3, IL-6, SCF and erythropoietin (EPO).

(C) Representative images of colonies of *WT/control* or *WT/sPrdm16* cells treated with vehicle or cytarabine.

(D) Cell cycle analysis of *WT/control* and *WT/sPrdm16* cells (n=3 for each group).

(E) Cell cycle analysis of *WT/sPrdm16* cells derived from colony forming assay treated with vehicle or cytarabine (n=3 for each group).

(F) In vitro drug sensitivity assay for cytarabine using *Flt3^{ITD}/control* and *Flt3^{ITD}/sPrdm16* (n=3 for each group).

(G) Colony forming assays with cytarabine (left panel) or daunorubicin (right panel) were performed using *Flt3^{ITD}/control* and *Flt3^{ITD}/sPrdm16* cells, which were plated in triplicate.

(H) Representative images of colonies of *Flt3^{ITD}/control* or *Flt3^{ITD}/sPrdm16* cells treated with vehicle or cytarabine.

(I) Cell cycle analysis of *Flt3^{ITD}/control* and *Flt3^{ITD}/sPrdm16* cells (n=3 for each group).

(J) Cell cycle analysis of *Flt3^{ITD}/sPrdm16* cells derived from colony forming assay treated with vehicle or cytarabine (n=3 for each group).

All data are represented as mean \pm standard deviation. An unpaired Student's t test was used to calculate p values. N.S., not significant; * <0.05 ; ** <0.01 ; *** <0.001 ; **** <0.0001 ; ***** <0.00001 .

Supplemental Figure 3. sPrdm16 activates oxidative phosphorylation in WT cells.

(A) GO terms of upregulated genes in *MA9/sPrdm16* cells compared to *MA9/control* cells (n=3 for each group).

(B) Differentially expressed genes in *WT/sPrdm16*. There were 1015 up-regulated genes, and 357 down-regulated genes.

(C) GO terms of upregulated genes in *WT/sPrdm16* cells compared to *WT/control* cells (n=3 for each group).

(D-E) The gene signatures significantly changed in GSEA using RNA-seq data from *WT/sPrdm16* vs *WT/control* cells (D). The gene signature related to "OXIDATIVE PHOSPHORYLATION" was significantly enriched in *WT/sPrdm16* cells (D-E).

(F) Mito Stress Test (left panel) and Glycolysis Stress Test (right panel) in *WT/control* and

WT/sPrdm16 cells (n=3 for each group).

Supplemental Figure 4. Metformin, tigecycline and IACS-010759 inhibit mitochondrial respiration in *MA9/sPrdm16* cells.

(A) Mito Stress Tests were performed using *MA9/sPrdm16* cells treated with AraC 500nM alone for 1 hour (left panel), metformin 1mM alone for 24 hours (middle panel), or a combination of cytarabine and metformin (right panel) (n=3 for each group).

(B) Mito Stress Tests were performed using *MA9/sPrdm16* cells treated with tigecycline 10μM alone for 24 hours (left panel), or a combination of cytarabine and tigecycline (right panel) (n=3 for each group).

(C) Mito Stress Tests were performed using *MA9/sPrdm16* cells treated with either vehicle, IACS-010759 100nM alone for 24 hours (left panel), or a combination of cytarabine and IACS-010759 (right panel) (n=3 for each group).

Supplemental Figure 5. *sPrdm16* induces metabolic reprogramming through the activation of glutaminolysis via Myc-Slc1a5 axis in *WT*, *MA9*, *MOLM-13* and *THP-1* cells.

(A) Metabolite concentrations in the TCA cycle of *MA9/control* or *MA9/sPrdm16* cells treated with cytarabine were measured using capillary electrophoresis time-of-flight mass spectrometry-based metabolome profiling (n=6 for each group).

(B) In vitro drug sensitivity assay for BPTES, a glutaminase inhibitor, using *MA9/control* and *MA9/sPrdm16* (n=3 for each group).

(C) The gene signatures related to “MYC-TARGET” were significantly enriched in *WT/sPrdm16* cells.

(D) Transcripts Per Million (TPM) values of *Slc1a5* (left panel) and *c-Myc* (right panel) genes were upregulated in *WT/sPrdm16* cells (n=3 for each group).

(E) Western blot analysis for sPRDM16, MYC, SLC1A5 and VINCULIN in MOLM13 and THP-1 cells transduced with either mock or *sPRDM16*-expressing retroviral vector. Immunoblots (left panel) and densitometry quantification of the immunoblot bands (right panel) are shown (n=3 for each group). Band density was quantified by Image J software.

(F-G) Intracellular glutamine and glutamate uptake levels, measured by Glutamine/Glutamate-Glo Assay, were higher in MOLM13/*sPRDM16* (F) and THP-1/*sPRDM16* cells (G) compared to control cells (n=3 for each group).

(H) Mito Stress Test in MOLM13/control and MOLM13/*sPRDM16* cells. Oxygen consumption rate (OCR) curve (left panel) and bar graphs of basal and maximal respiration at the earliest timepoint in each phase (right panel) are shown (n=4 for each group).

(I) Mito Stress Test in THP-1/control and THP-1/*sPRDM16* cells. OCR curve (left panel) and bar graphs of basal and maximal respiration at the earliest timepoint in each phase (right panel) are shown (n=5 for each group).

All data are represented as mean \pm standard deviation. An unpaired Student's t test was used to calculate p values. N.S., not significant; * <0.05 ; ** <0.01 ; *** <0.001 ; **** <0.0001 .

Supplemental Figure 6. Myc regulates glutaminolysis and mitochondrial respiration.

(A) Intracellular glutamine and glutamate uptake levels were decreased in *MA9/sPrdm16* cells transduced with shRNA #1 (left panels) or #2 (right panels) against Myc compared to scramble-transduced cells (n=3 for each group).

(B) Mito Stress Test of *MA9/sPrdm16* cells transduced with either scramble, shRNA #1 (left panel) or #2 (right panel) against Myc (n=3 for each group).

(C) The 3D synergy maps showing the synergistic effects of a combination of cytarabine and 10058-F4, a Myc inhibitor, on *MA9/control* (upper panel) or *MA9/sPrdm16* (lower panel) cells. The regions indicating synergistic or antagonistic effects are represented in red and blue, respectively.

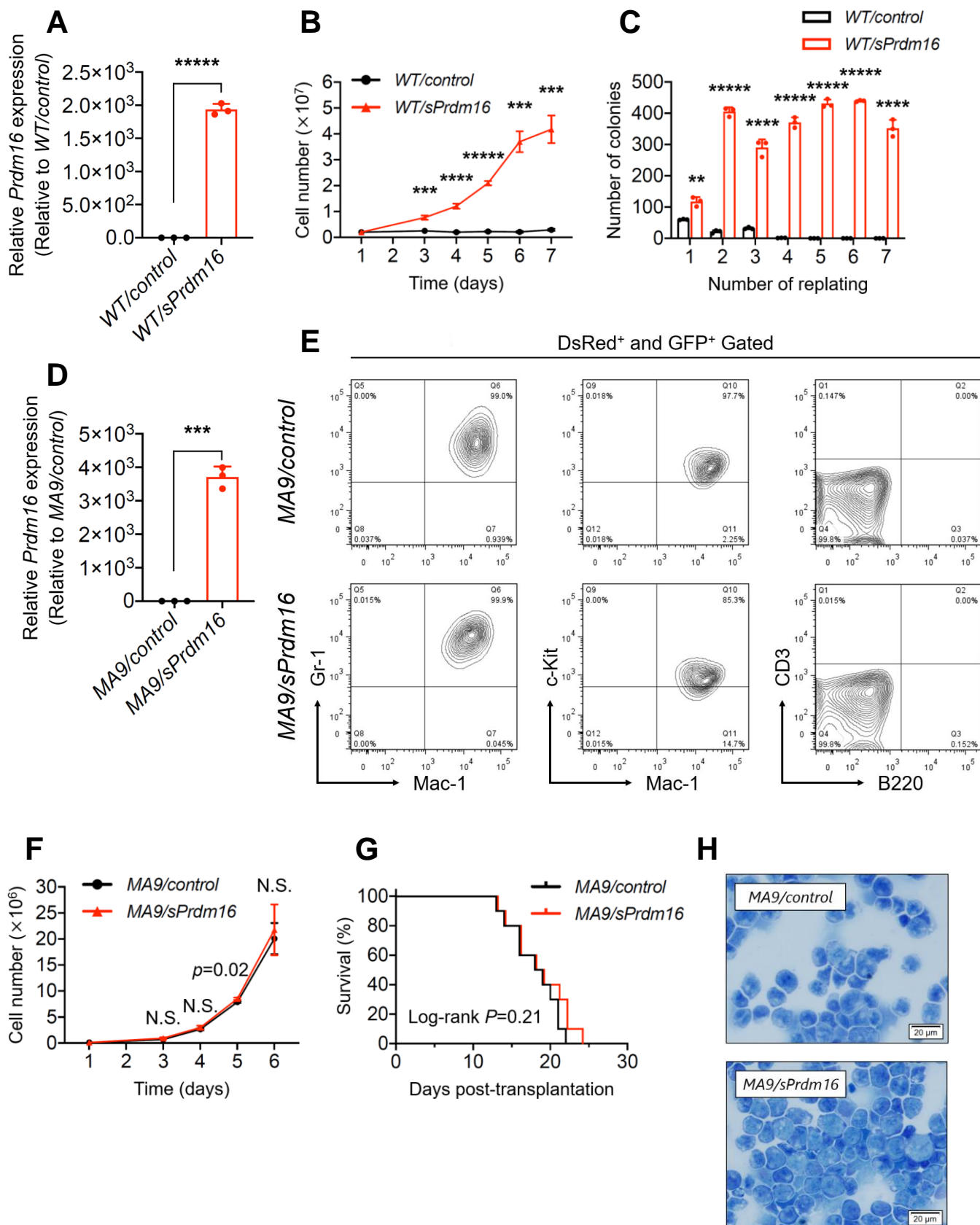
(D) Intracellular glutamine (left panel) and glutamate (right panel) uptake levels were increased in *MA9/Myc* cells compared to *MA9/control* cells (n=3 for each group).

(E) Mito Stress Test in *MA9/control* and *MA9/Myc* cells (n=3 for each group).

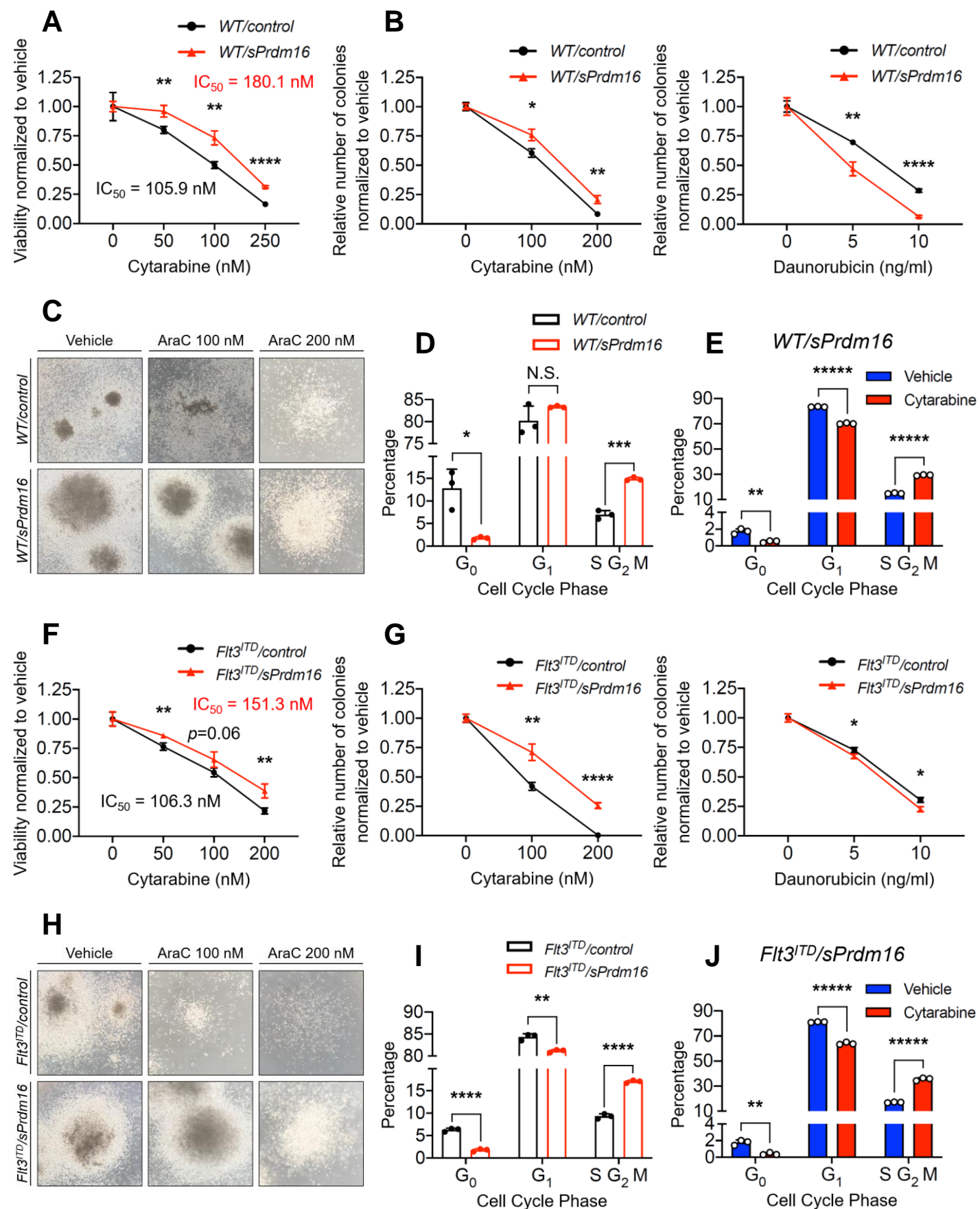
(F) Mitochondrial reactive oxygen species (ROS) and membrane potential in *MA9/Myc* cells were measured using MitoSOX and the ratio of tetramethylrhodamine methyl ester (TMRM) and mitotracker, respectively (n=3 for each group).

All data are represented as mean \pm standard deviation. An unpaired Student's t test was used to calculate p values. * <0.05 ; ** <0.01 ; *** <0.001 ; **** <0.0001 ; ***** <0.00001 .

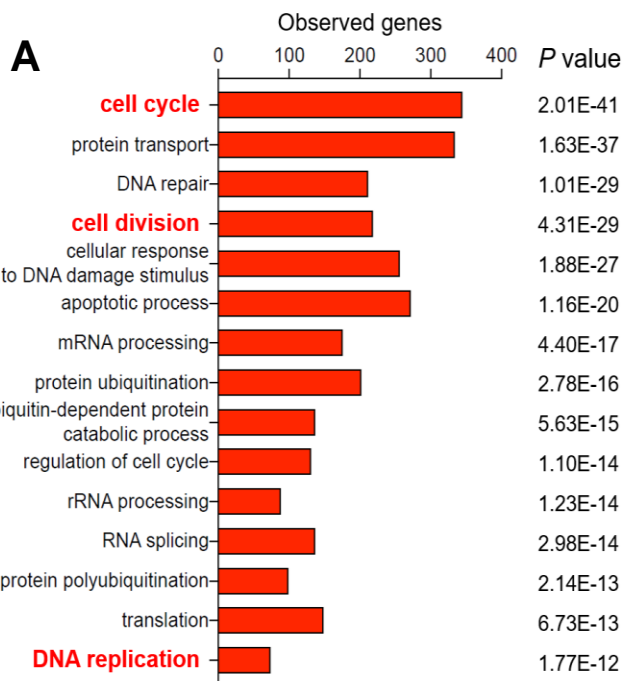
Supplemental Figure 1



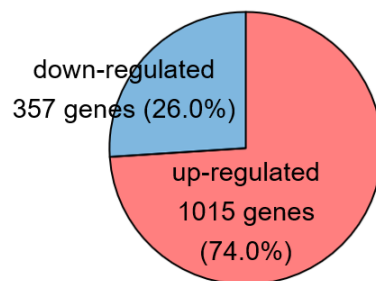
Supplemental Figure 2



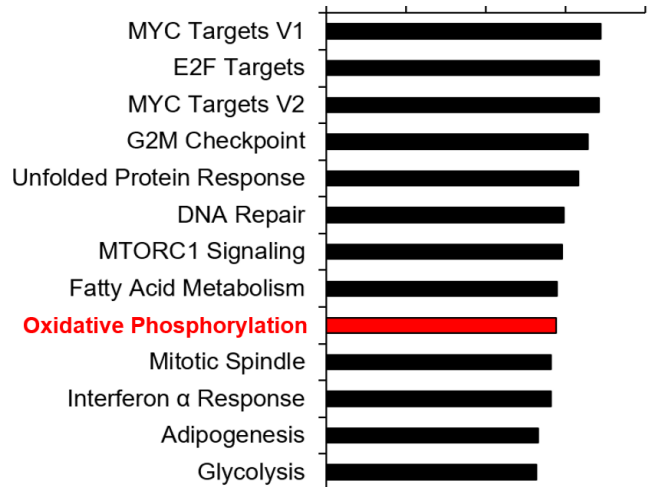
Supplemental Figure 3



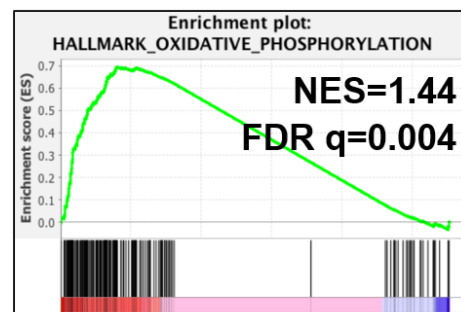
B *WT/sPrdm16*



D Normalized Enrichment Score

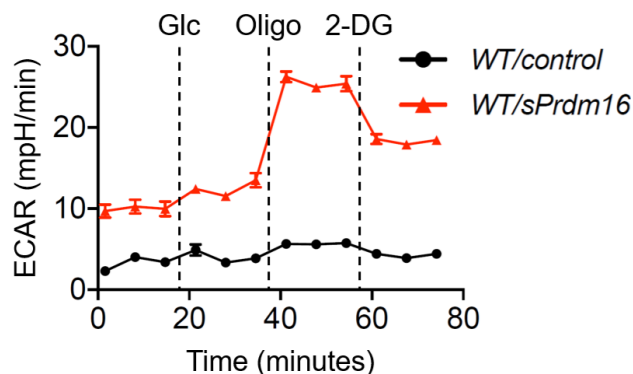
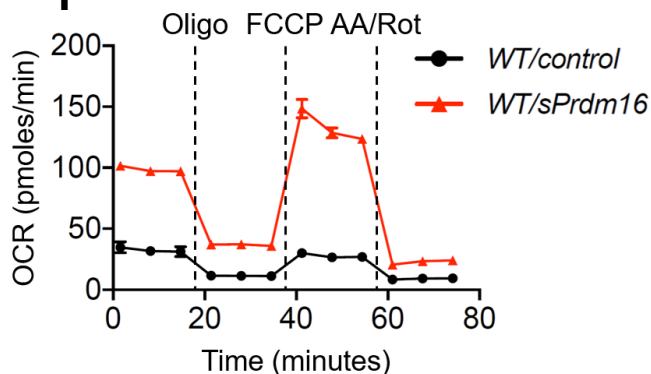


E

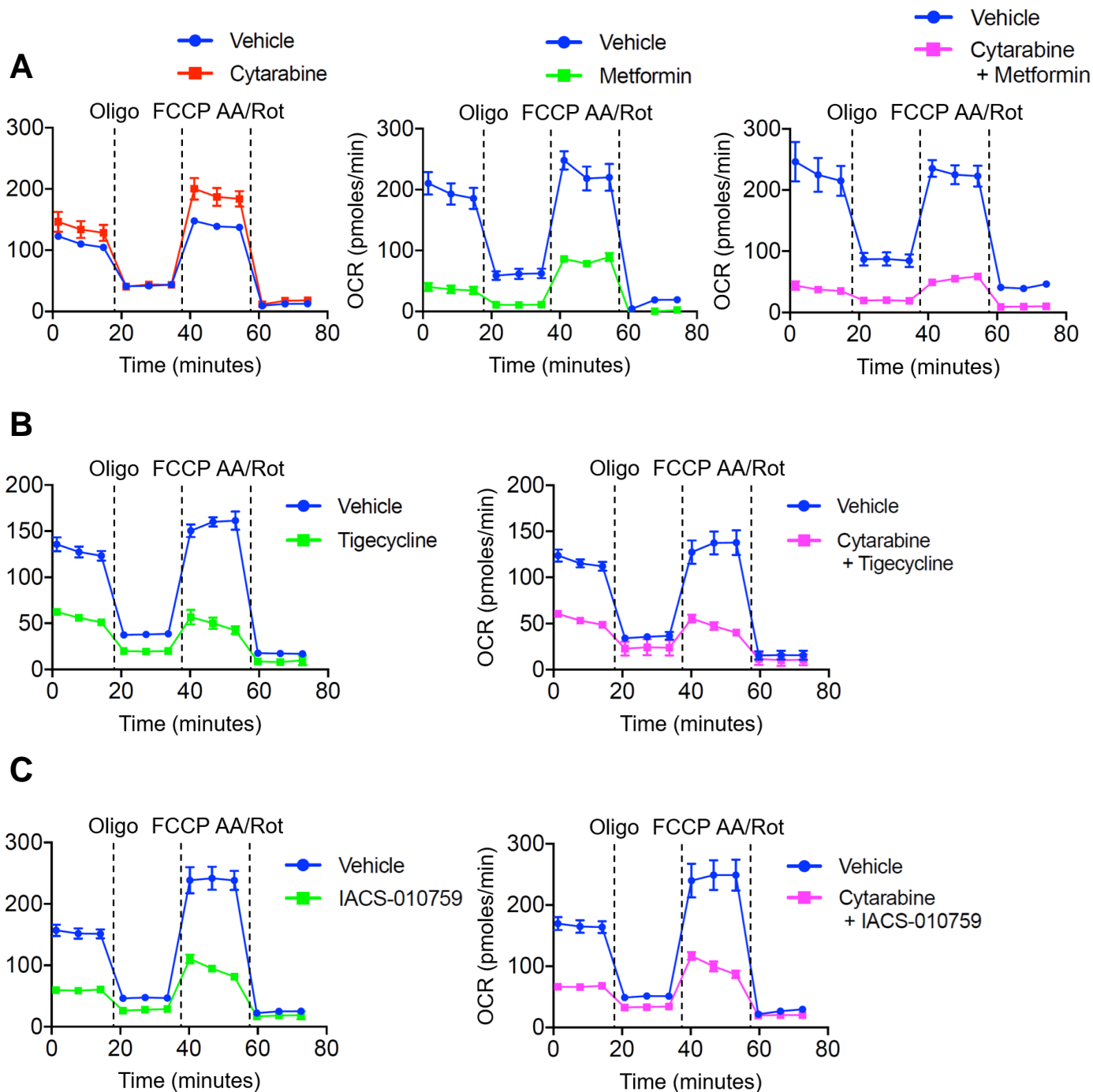


WT/sPrdm16 *WT/control*

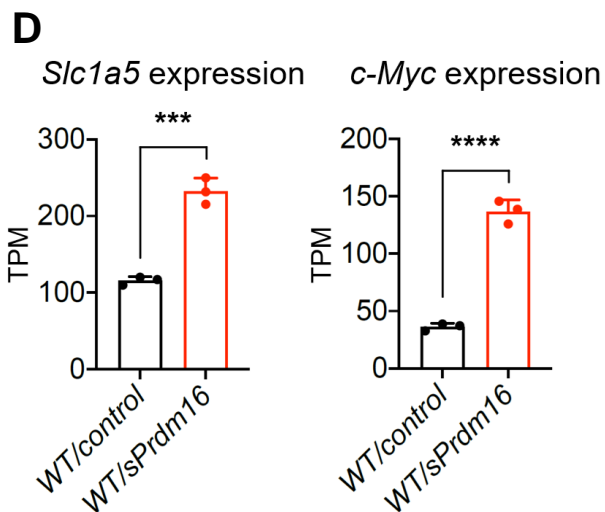
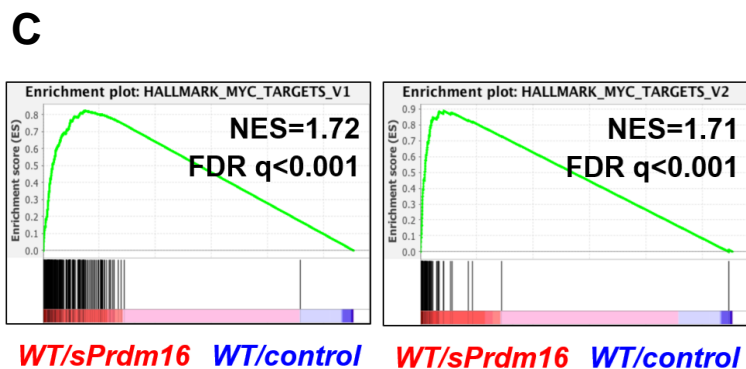
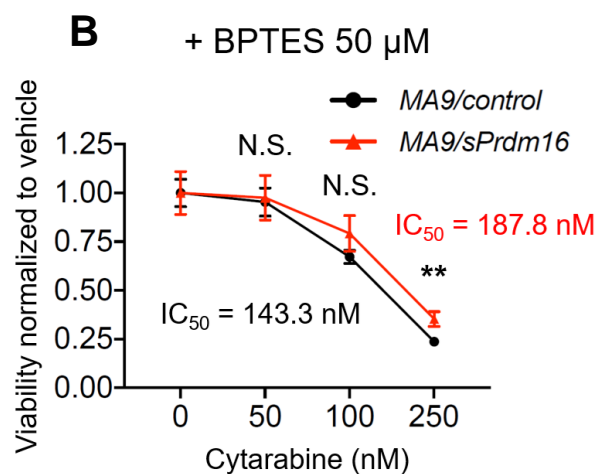
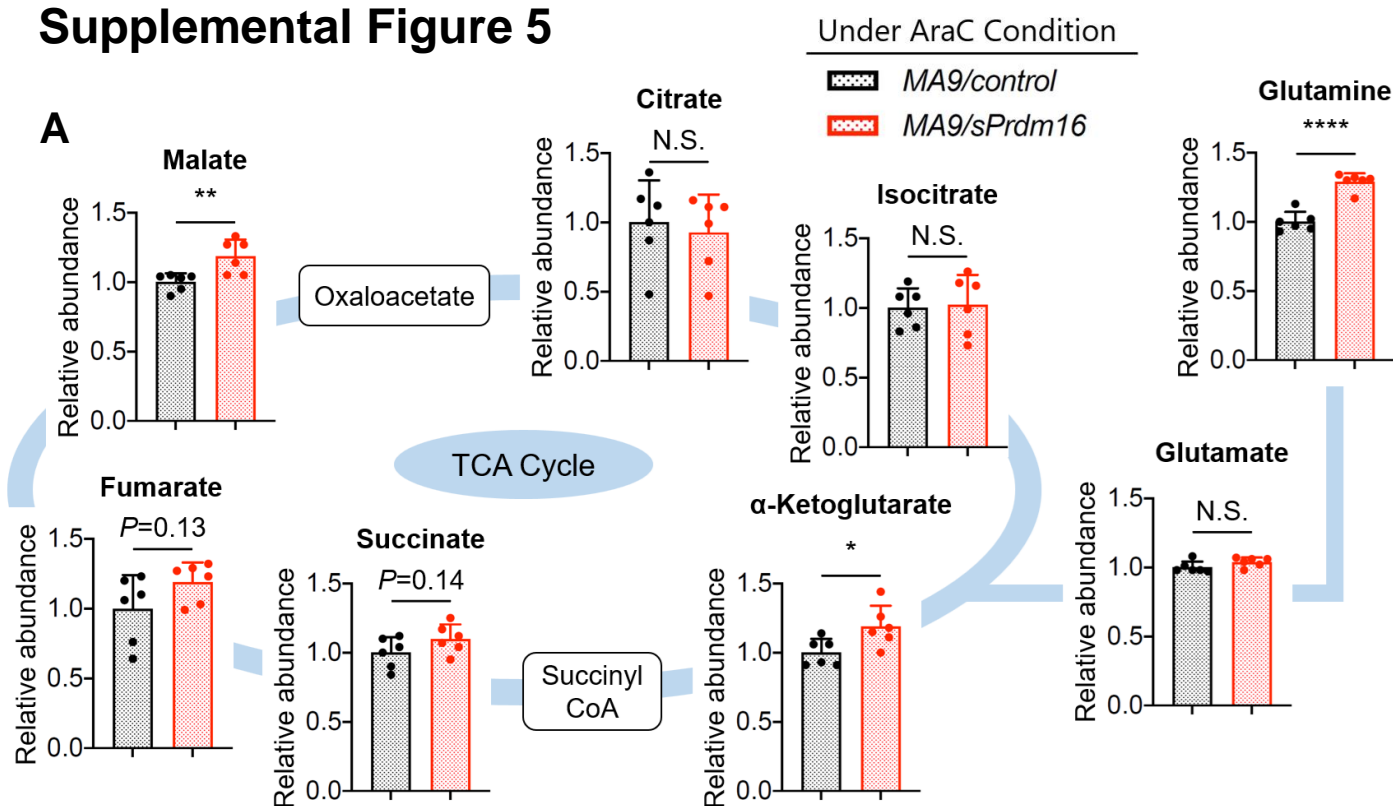
F



Supplemental Figure 4

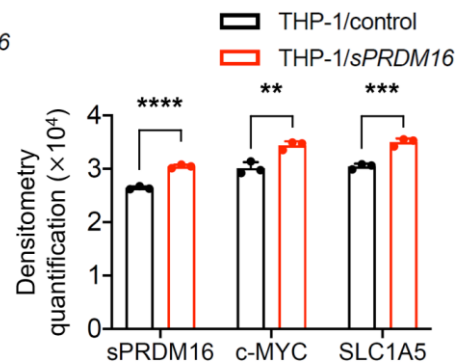
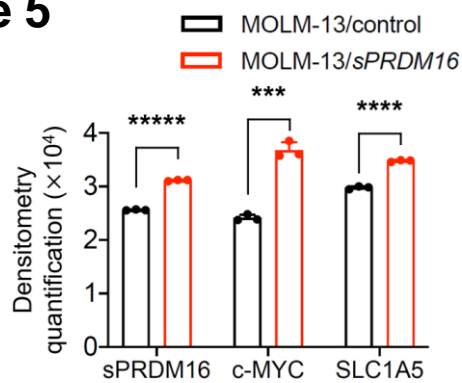
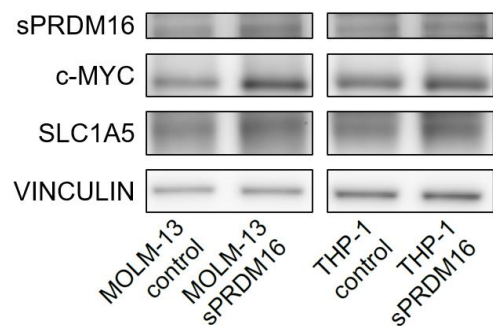


Supplemental Figure 5



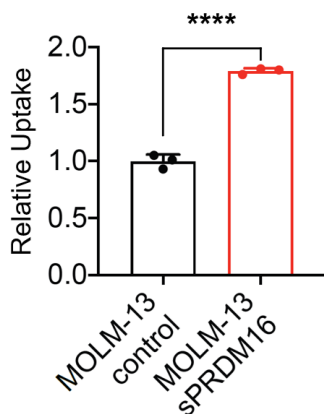
Supplemental Figure 5

E

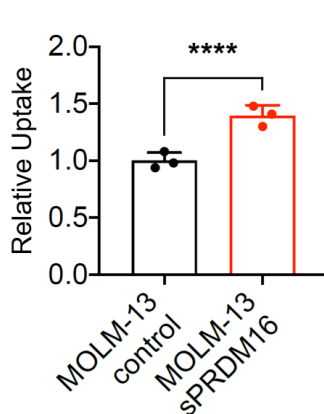


F

Glutamine

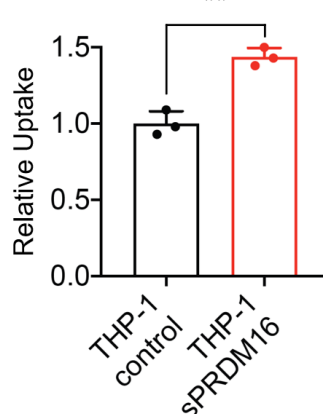


Glutamate

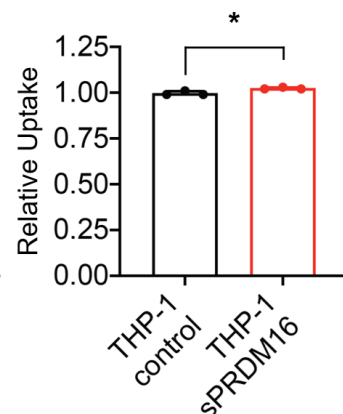


G

Glutamine

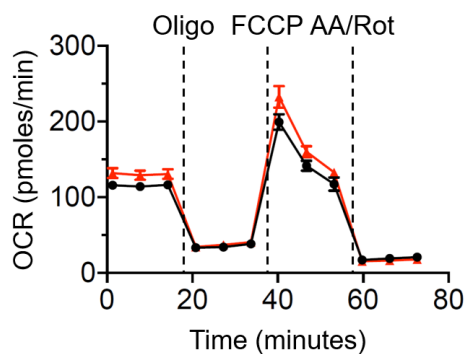


Glutamate

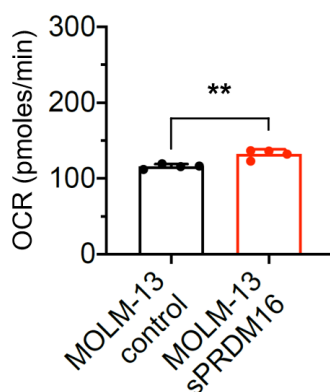


H

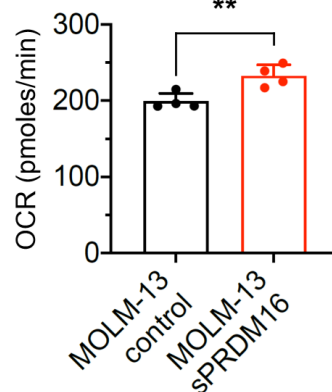
● MOLM-13/control
▲ MOLM-13/sPRDM16



Basal Respiration

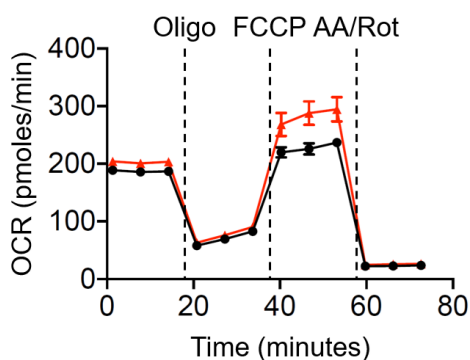


Maximal Respiration

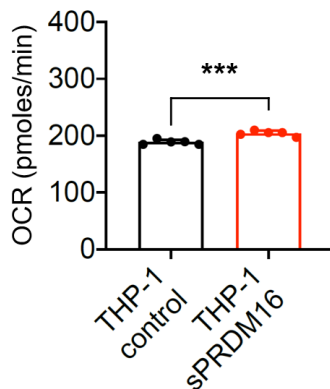


I

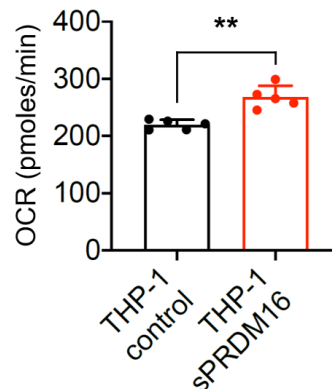
● THP-1/control
▲ THP-1/sPRDM16



Basal Respiration



Maximal Respiration



Supplemental Figure 6

